Biomolecular Detection and Quantification 14 (2017) 7–18

Contents lists available at ScienceDirect

Biomolecular Detection and Quantification

journal homepage: www.elsevier.com/locate/bdq

Research paper

Amplification of nonspecific products in quantitative polymerase chain reactions (qPCR)

Adrián Ruiz-Villalba[a,b], Elizabeth van Pelt-Verkuil[c], Quinn D Gunst[a], Jan M Ruijter[a], Maurice JB van den Hoff[a,*]

[a] Academic Medical Center, Department of Medical Biology, Meibergdreef 15, 1105AZ Amsterdam, The Netherlands
[b] Foundation of Applied Medical Research (FIMA), Area of Cell Therapy, University of Navarra, Avd Pío XII, 36 − 31008, Pamplona, Spain
[c] Department of Innovative Molecular Diagnostics, University of Applied Sciences, Leiden, The Netherlands

ARTICLE INFO

Handled by Jim Huggett

Keywords:
RT-qPCR
Melting curve analysis
Reaction parameters
Artifacts

ABSTRACT

Quantitative PCR allows the precise measurement of DNA concentrations and is generally considered to be straightforward and trouble free. However, a survey with 93 validated assays for genes in the Wnt-pathway showed that the amplification of nonspecific products occurs frequently and is unrelated to C_q or PCR efficiency values. Titration experiments showed that the occurrence of low and high melting temperature artifacts was shown to be determined by annealing temperature, primer concentration and cDNA input. To explore the range of input variations that occur in the normal use of the Cre assay these conditions were mimicked in a complete two-way design of template −plasmid DNA- and non-template −mouse cDNA- concentrations. These experiments showed that the frequency of the amplification of the correct product and the artifact, as well as the valid quantification of the correct product, depended on the concentration of the non-template cDNA. This finding questions the interpretation of dilution series in which template as well as non-template concentrations are simultaneously decreasing. Repetition of this cDNA concentration experiment with other templates revealed that exact reproduction qPCR experiments was affected by the time it takes to complete the pipetting of a qPCR plate. Long bench times were observed to lead to significantly more artifacts. However, the measurement of artifact-associated fluorescence can be avoided by inclusion of a small heating step after the elongation phase in the amplification protocol. Taken together, this trouble-shooting journey showed that reliability and reproducibility of qPCR experiments not only depends on standardization and reporting of the biochemistry and technical aspects but also on hitherto neglected factors as sample dilution and waiting times in the laboratory work flow.

1. Introduction

Quantitative PCR, qPCR or RT-qPCR, allows the sensitive, rapid and precise measurement of DNA or RNA targets. The method is used for e.g diagnostic purposes, gene expression studies for a restricted panel of genes in fundamental and translational research and validation of transcriptome analyses. In general, qPCR is considered to be straightforward and trouble free. As a consequence, most papers do not report the optimization and validation carried out to determine the specificity and sensitivity of an assay [1] although the MIQE guidelines specifically ask for such proof [2]. Optimization of qPCR is performed to avoid off-target products and artifacts. This optimization is commonly carried out with negative and positive control samples; the loss of specific product in a dilution series of the positive sample is then considered to indicate the lower detection limit of the assay [3]. For reactions with high C_q values, it is generally recommended to check the identity of the amplified product with melting curve, size and/or sequence analysis. Unnoticed amplification of a nonspecific product (artifacts), results in false positive results and underlines the emphasis of the MIQE guidelines on assay specificity.

Amplification artifacts can be shorter or longer than the intended amplicon. Short artifacts are most often primer dimers, which are mainly due to homology between the primers sequences [4]. Long artifacts comprise off-target products which contain additional sequences that do not or only partially overlap with the targeted sequence [5]. Although some papers describe how to prevent amplification of non-specific products [6–8], hardly any paper deals with the conditions leading to these off-target products.

The replacement of a 1-step RT-qPCR protocol by a 2-step protocol (cDNA synthesis followed by separate PCR reactions) reduces the occurrence of primer-dimers in the no-template control [9]. The 2-step protocol allows a better control of the temperature during the phase of

* Corresponding author at: Academic Medical Center, Department of Medical Biology, Meibergdreef 15, 1105AZ Amsterdam, The Netherlands.
E-mail address: m.j.vandenhoff@amc.uva.nl (M.J. van den Hoff).

http://dx.doi.org/10.1016/j.bdq.2017.10.001
Received 11 July 2017; Received in revised form 3 October 2017; Accepted 5 October 2017
Available online 01 November 2017

the cycling protocol in which primers anneal to the available DNA strands and each other [10]. Hot-start PCR prevents primer extension due to interactions between reaction components at low temperature prior to the first denaturation step of the cycling protocol [6,7,11] and is therefore considered to reduce artifact formation. When these extended primers share homology with a sequence elsewhere in the genome, a phenomenon dubbed "jumping" can occur [12]. In such a within-genome recombination a completely new product is amplified [12,13]. The frequency of jumping is suggested to depend on the ratio of template to non-template DNA rather than on the absolute concentration of the template [14].

In this study we describe a series of trouble-shooting experiments that was done to get to grip on the conditions in which PCR artifacts occur in reactions with validated assays on the sample type for which they were designed. These analyses showed that the balance between primer, template and non-template concentrations determines whether the correct product and/or an artifact will be amplified. Qualitatively, low template concentrations increase artifact frequency whereas, quantitatively, low non-template concentrations lead to deviating C_q values and thus to incorrect quantification. Moreover, the occurrence of artifacts was shown to be highly dependent on the time it took to complete the pipetting of the qPCR plate despite implementation of a hot-start procedure. Measurement of the fluorescence at a temperature above the Tm of the primer-dimers was shown to give the expected results despite the formation of artifacts. These observations show that low-input gene expression experiments of a complicated design have to be carefully optimized, standardized, performed and evaluated, especially when 'not expressed' or 'not present' are among the possible outcomes.

2. Material and methods

2.1. Primer design

The PCR primers for genes in the Wnt pathway were designed using Primer-Blast (NCBI). The following criteria were taken into account when designing the primer pairs: (1) each primer should be 19–22 bp in length, (2) the annealing T_m should be 60 ± 1 °C, (3) the difference between the T_m of the two primers in a pair should be ≤ 1 °C, (4) the primers should have limited similarity with other sequences in the genome and especially not in the last 4 bases at the 3′ end of the primer [15] and (5) the amplicon should be between 70 and 150 bp in length. In addition, we aimed at primers that are exon–exon spanning, or that the amplicon is spanning an intron of at least 500 bp. However, this latter criterion could not be met for several targets, because many genes of the Wnt signaling pathway are without intron. Next the primers were analyzed using Oligoanalyzer v3.1 (IDT) with as analysis parameters: oligo-concentration: 1 μM, 50 mM Na^+, 2 mM Mg^+ and 0.25 mM dNTP. We aimed at primer pairs for which the homo-dimer and hetero-dimer strength is ΔG≤ −9 kcal/mol. Moreover, we checked that there are no extendable 3'ends in these home and hetero-dimers. Finally, we aimed at a T_m ≤ 55 °C of the primer-dimers.

The target specificity of the designed primer pairs was tested in qPCR reactions with cDNA of complete chicken embryos as positive control tissue. As negative controls we used minus-RT and no-tissue control (NTC) reactions. A reaction with genomic DNA served to determine cDNA specificity. After the PCR reaction the amplification curve was inspected with respect to background and plateau level (ratio ≥ 10), as well as the PCR efficiency (> 1.7; Fig. 1C). After the qPCR run, we performed melting curve analysis, gel electrophoresis and sequencing to verify that the expected target was amplified. If this verification failed an alternative primer pair was designed and tested. The primer pairs that were used in the reported analysis are shown in Supplemental Table 1.

MS2 primers were obtained both from literature [16] or designed (Supplemental Table 2) using Allele ID (PREMIER Biosoft). Primer pairs were evaluated *in silico* and using dilution series, gradient PCRs and checkerboard titrations.

The primers used to amplify the 341 bp Cre amplicon were; forward primer: GGTTCGCAAGAACCTGATGGACAT and reverse primer: CTAGAGCCTGTTTTGCACGTTCA [17].

2.2. Experiments with chicken embryos

Fertilized chicken eggs were obtained from a local hatchery (Drost BV, Nieuw Loosdrecht, the Netherlands) and incubated for three days at 38 °C. The embryonic tissue around the developing heart was divided into five regions. Samples were collected in TriReagent® (Life Technologies) and total RNA was immediately isolated; RNA purity and quantity were determined using the Nanodrop. Per RT-reaction 300–1000 ng of total RNA was converted into cDNA using anchored oligo-dT primers (T_{14}VV) and Superscript II reverse transcriptase (Life Technologies). Each 10 μL qPCR reaction contained an amount of cDNA equivalent to 5 ng of total RNA (5 RNA equivalents), *LightCycler® 480 SYBR Green I Master mix* (Roche), and 1 μM of the forward and reverse primer. The qPCR was run in a *LightCycler® 480 Multiwell Plate 384* cycler (Roche): 5 min 95 °C followed by 45 cycles 10 s 95 °C, 20 s 60 °C and 20 s 72 °C, and a melting curve analysis to verify the amplification product. Negative controls were (i) a no-tissue control (NTC; water) and (ii) a RT-reaction without enzyme. As positive control 5 RNA equivalents of cDNA prepared from entire chicken embryos was used. The expression level of 93 genes related to Wnt signaling and two reference genes was measured in triplicate per tissue.

2.3. Experiment with MS2 virus

The enterobacteriophage MS2 (DSM No 13767; strain PC-V3463; Genbank NC_001417) and *Escherichia coli* host cells (DSMZ 5695) were purchased (Leibniz Institute DSMZ-German Collection of Microorganisms and Cell Cultures, Braunschweig). A stock of MS2 was prepared of 4.8×10^{10} PFU per mL. The MS2 genome was isolated using the NucliSENS miniMAG kit (bioMérieux; Benelux, Zaltbommel, Netherlands) and after treatment with DNase converted into cDNA using the QuantiTect Reverse Transcription Kit (Qiagen). The cDNA was used undiluted (approx. 2×10^6 PFU) or diluted in 10-fold steps down to 10^{-10} and analyzed in 20 μL reactions using iQ™ Supermix (Biorad) or SsoFast™ EvaGreen® Supermix (Biorad) and primers at various concentrations in checkerboard designs. The qPCR was run in a BioRad CFX96™touch Real-time PCR detection system: 10 min 95 °C followed by 50 cycles of 15 s 95 °C and 1 min 60 °C, and a melting curve analysis to verify the amplification of the correct product. Each PCR variable was tested in one or more runs to reach at least triplicate measurements

2.4. Template/non-template checkerboard experiments

These experiments were carried out to evaluate the effect of the relative concentration of template versus non-template DNA in the reactions. A plasmid (pDNA) containing the sequence of *Cre* recombinase enzyme [17] was used as template. cDNA from hearts of newborn mice served as non-template DNA. RNA and cDNA preparation and PCR reaction were as described in the above chicken experiment. The input of the reactions consisted of a complete checkerboard design with all combinations of template (10-times dilution series from 15.10^3 down to 1.5 and 0 copies of pDNA) and non-template (5-times dilution series from 10 down to 0.0032 and 0 ng RNA equivalents of cDNA) concentrations. Note that this two-way design encompasses the range of variations in cDNA and target concentrations that occurs in a (dilution) series of different tissues for which the Cre-assay was designed. The experiment was replicated in 2 PCR runs and carried out with 2 primer concentrations (1 μM and 0.1 μM) with four technical replicate reactions per combination of inputs.

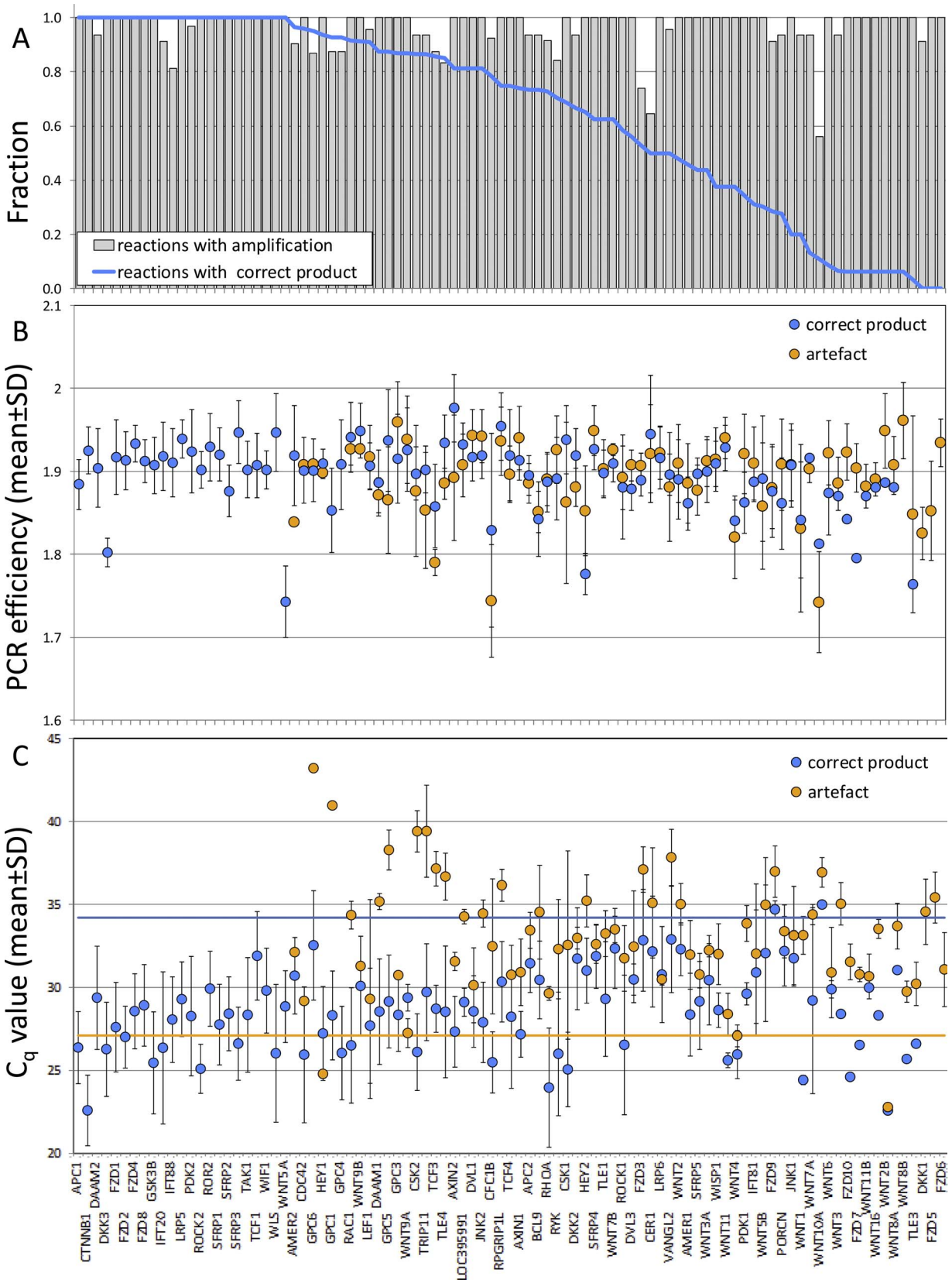

Fig. 1. Frequency of occurrence of artifacts and their relation to the PCR efficiency and C_q value. The frequency at which PCR artifacts occur was determined for 93 genes of interest (Supplemental Table 1) of which the expression levels were determined in triplicate in 5 different tissues involved in the development of the chicken heart. **A**: the fraction of qPCR reactions in which amplification was observed (bar graph) and the fraction of those reactions that showed the correct PCR product based on melting curve analysis (line graph). **B**: PCR efficiency of the reactions leading to the correct amplification product (blue circles) or a nonspecific artifact (orange circles). **C**: C_q values of the reactions leading to the correct amplification product (blue circles) or a nonspecific artifact (orange circles). The horizontal blue line is the upper 95% confidence level (CI) of the C_q values of the correct reactions whereas the orange horizontal line is the lower 95% CI of the C_q values of the artifacts. In all panels genes are ordered by decreasing fraction of reactions with amplification of the correct product. Bars show mean ± SD. (For interpretation of the references to colour in this figure legend, the reader is referred to the web version of this article.)

2.5. Time-on-bench experiment

In the 'time-on-bench' experiment, the template/non-template experiment was carried out in such a way that after completely pipetting each of three sets of reactions the 384-well plate was left on the bench at room temperature for 3, 2 and 1 h. In an additional pre-incubation experiment the master mix and the primers were mixed and left on the bench for 2.5 h before the template and non-template mixtures were added. The latter set-up reproduced the pipetting scheme of the above checkerboard experiments. Template pDNA concentrations ranged from 150000 to 1.5 molecules whereas the non-template cDNA concentrations decreased in parallel from 1 to 10^{-5} ng RNA equivalents. The experiment was performed with technical triplicates.

2.6. Fluorescence measurements

A full template/non-template checkerboard experiment as described above was carried out with standard measurement of SYBR Green fluorescence immediately after the elongation phase at 72 °C. However, in the PCR protocol a fourth segment was introduced in every cycle to allow a second fluorescence measurement after increasing the plate temperature to 82 °C. The latter temperature is above the Tm of the primer-dimers and thus enables measurement of only the fluorescence of the desired product [18,19]. At both temperatures the characteristics of the amplification curves were determined and the starting concentrations were calculated. Melting curve analysis was performed to determine which product(s) were amplified. This experiment was carried out twice with four technical replications.

2.7. Quality controls and data analysis

Melting curve analysis provided by the cyclers was carried out for all reactions in all experiments and used to compare the melting peak of the amplified products to those observed in positive and negative controls. The size of the products was determined using 2-2.5% agarose gels and was confirmed by sequencing. The raw fluorescence data was exported from the qPCR machines. Baseline correction and analysis of the amplification curves was done with *LinRegPCR* [20,21]. C_q values, PCR efficiency values and target quantities (N_0) per assay are given in the (supplemental) results. Inter-run variation in the duplicate experiments was determined and removed using the *Factor-qPCR* program [22]. *SPSS* (version 23, IBM) was used for statistical analyses.

3. Results

3.1. Frequency of occurrence of PCR artifacts

Primers for 93 genes associated with the Wnt-pathway were designed and validated with established criteria for technical sensitivity and specificity. A mixture of entire chicken embryos, expressing all 93 genes served as positive sample. Moreover, a minus-RT and a no-tissue control sample were used as negative controls. In the positive control, the qPCRs showed only the expected product, based on agarose gel electrophoresis, melting curve analysis and sequence analysis, and no product or artifact in any of the negative control samples. These validated primer sets were used to analyse the expression, if any, of these 93 genes in triplicate in cDNA derived from 5 different parts of the embryonic chicken heart that express these genes at different levels. Amplification curve analysis, showed that for 64 genes all reactions resulted in an amplification product (Fig. 1A, Supplemental Fig. 1A, bars). For 29 genes between 97 and 55% of the reactions per assay showed an amplification curve that reached the plateau. However, melting curve analysis showed that only for 23 assays all reactions amplified the correct product. In the remaining assays some reactions either an artifact or both an artifact and the correct product were amplified. The finding of aberrant products was independent of the fraction of reactions that showed amplification (Fig. 1A, Supplemental Fig. 1A, line graph). Analysis of the amplification curves showed that the amplification efficiency of the reactions resulting in correct product and those resulting in artifacts (Fig. 1B) did not differ systematically ($p = 0.488$); for 6 genes the artifact showed a higher and for 4 genes a lower PCR efficiency (Supplemental Fig. 1B). The expression level differed per gene and per analyzed cardiac compartment with the upper 95% confidence limit of the C_q values for the correct product at 34.2 (Fig. 1C). Although the C_q values of reactions that resulted in artifacts were systematically higher than those of the correct product for the same gene ($p < 0.001$; Supplemental Fig. 1C) these reactions showed an overlapping range of C_q values with a lower 95% confidence limit of 27.1 (Fig. 1C). These results from a dataset with 93 assays show that amplification of nonspecific products occurs frequently and that amplification of these products cannot simply be identified from a deviating PCR efficiency or a high C_q value, indicated by the slopes and the positions of the amplification curves, respectively. Although for some assays correct products are amplified with high C_q values, C_q values above 34 almost certainly point to an artifact. However, because 5% of the artifacts were formed with C_q values below 27 and 5% of the correct products took 34 or more cycles to reach the quantification threshold setting, fixed C_q criteria for judging reaction performance and assay outcome cannot be set.

3.2. Types of nonspecific PCR products

Phage MS2 is frequently used as internal process control in diagnostic assays of RNA viruses. Its simple genome and validated primers provide an ideal model to study the occurrence of artifacts by qPCR reaction conditions and the influence of pro- or eukaryotic cDNA of whatever tissue type. The MS2 assay was used in dilution and titration experiments to study the conditions that lead to the amplification of artifacts. The specific PCR product of this assay has a melting temperature of 81.5 °C (Fig. 2A; open triangles). A series of dilution experiments showed that at low cDNA input ($< 10^{-5}$ dilution corresponding to less than 20 PFU per reaction) the reaction either failed or led to a low melting temperature product (< 78 °C; Fig. 2A; filled triangles). However, in some of the reactions with high MS2 input a nonspecific product with a high melting temperature (84 °C) was found (Supplemental Fig. 2).

The sporadic occurrence of the correct amplicon in the most diluted samples (Fig. 2A; open circles) shows that under those conditions the presence of the target molecules is determined by Poison probability. Therefore, the increasing variation in C_q values in the 10^{-5} dilution (about 20 PFU) and in the more diluted samples reflects the increasingly random presence of target molecules in the reaction at C_q values above 35 [23].

Varying the annealing temperature in reactions with the no-template control (NTC) or the 10^{-2} diluted (about 20,000 PFU) MS2 input showed that at lower annealing temperatures the occurrence of low melting temperature artifacts increased in the NTC input, whereas at higher temperatures the high melting temperature artifacts appeared in the 10^{-2} diluted MS2 input (Fig. 2B). Gel electrophoresis showed corresponding bands in both conditions (data not shown). Sequencing showed that the latter product consisted of a rearranged sequence of the MS2 genome.

Varying the primer concentration in reactions with the NTC or the 10^{-2} diluted MS2 input showed a similar diversity of products (Fig. 2C). The relatively high 10^{-2} diluted MS2 input was chosen deliberately in order to enhance the effects of the primer concentration. The lowest primer concentration did not result in a product in either input. Increasing the primer concentration in NTC samples showed an increase in the occurrence of a low melting temperature artifact. The high melting temperature artifact occurred more often in the reactions with the highest primer concentrations.

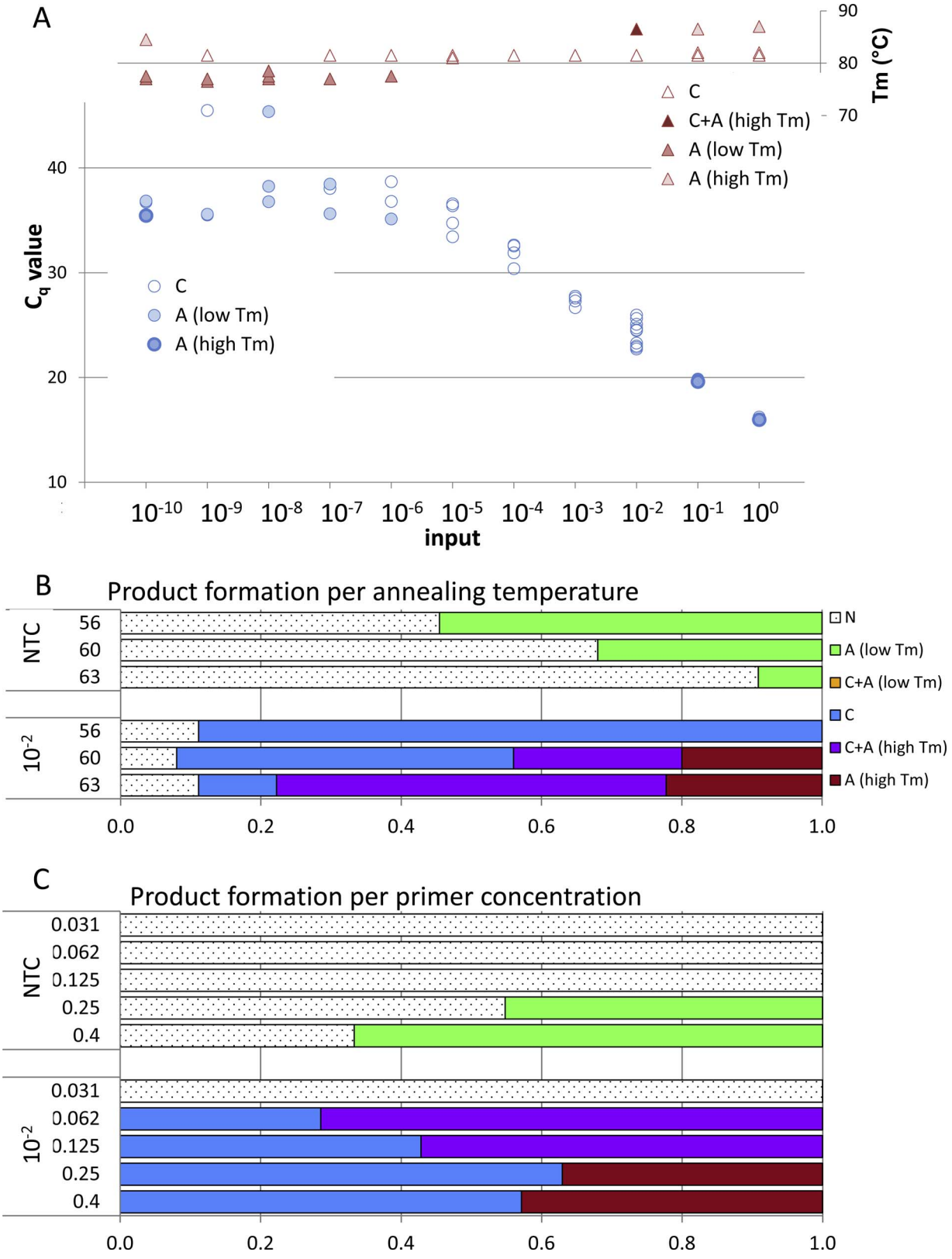

Fig. 2. Identification of different types of nonspecific PCR products. In a dilution series of MS2 template different PCR artifacts occur. **A**: C_q value (left Y-axis) and the melting temperature of the amplification product (right Y-axis) of each PCR reaction at each dilution of input MS2 DNA. Melting curve analysis showed reactions with the correct product (C), an artifact (A) or both. The shading of a marker indicates whether the melting profile showed one or two peaks and whether the melting temperature is equal (white), lower (light) or higher (dark) than the one of the targeted product. MS2 was targeted with the Dreier primers (Supplemental Table 2). **B**: Artifact formation with different annealing temperatures in the qPCR reaction of the no-tissue control (NTC) or 10^{-2} diluted MS2 template. **C**: Artifact formation with different primer concentrations in the qPCR reaction mixture of the NTC or 10^{-2} diluted MS2 template. Experiments in panels **B** and **C** were performed with the FW947 – REV1050 primer pair (Supplemental Table 2).

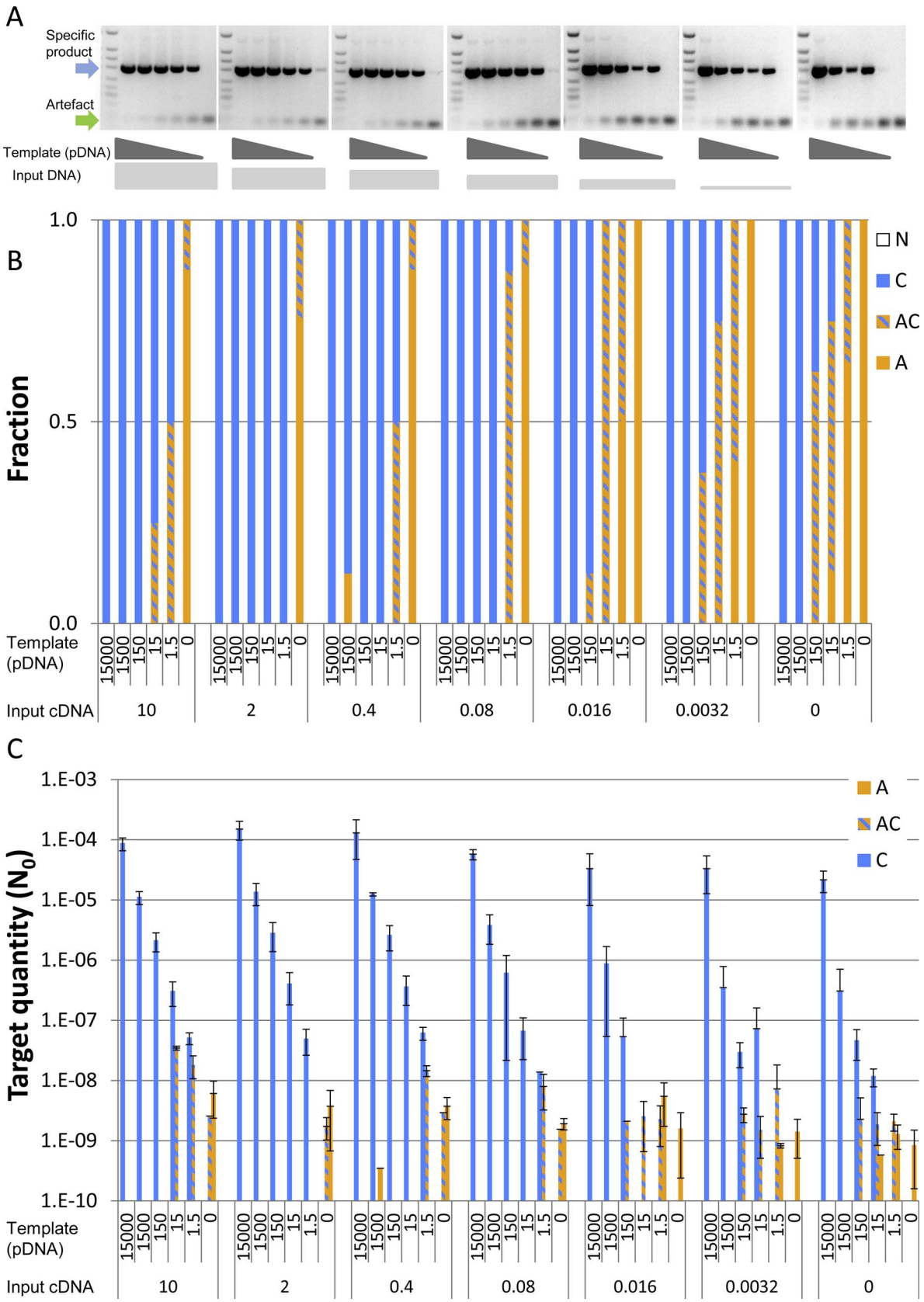

Fig. 3. Effects of template and non-template concentration on amplification. This experiment served to determine the combined effects of a 10-fold dilution of template plasmid DNA and a 5-fold dilution of non-template cDNA concentrations on the amplification results. **A**: Agarose gel analysis per group of reactions with a 10-fold dilution of the pDNA (dark grey triangle) per non-template cDNA concentration (light grey rectangle). Based on melting peak analysis (Supplemental Fig. 3) the reactions are grouped into those resulting in correct product (C), artifact (A), both products (AC), and no amplification (N). **B**: Fraction of PCR reactions per amplification product per template (pDNA) input within each non-template (cDNA) input. **C**: Observed target quantities per amplification product per template pDNA input within each non-template cDNA input. Bars show mean ± SD.

3.3. Effects of template and non-template DNA concentration

To discriminate between the effects of template and non-template input concentrations on the result of the amplification reaction an experiment with a complete two-way design of combined template (pDNA: plasmid DNA containing the Cre sequence) and non-template cDNA (cDNA of a whole mouse embryo that does not express Cre) concentrations was performed. Product size verification on agarose gels showed the amplification of the correct product, a small artifact or both products (Fig. 3A). Similarly, the melting peak analysis showed the correct peak (at 85.5 °C), the artifact (at 78.5 °C) or both (Supplemental Fig. 3A). On average the PCR efficiency values derived from the amplification curves [20] of individual reactions that resulted in the correct product were lower than those that resulted in the artifact or both products ($p < 0.001$) but the distribution of PCR efficiency values overlapped completely (Supplemental Fig. 3B). Within the set of reactions that resulted in the correct product there was no significant effect of template and non-template DNA concentration on the amplification efficiency ($p = 0.475$ and $p = 0.065$, respectively; Supplemental Fig. 3B). The occurrence of artifacts was determined by the input of template as well as non-template DNA (Fig. 3B). The highest cDNA concentration (10 RNA equivalents) resulted in amplification of artifacts in reactions with 15 pDNA copies or less. The occurrence of artifacts decreased at 2 and 0.4 RNA equivalents of non-template cDNA to increase again with lower concentrations. The highest template concentrations always resulted in the correct product and without input of template only the 78.5 °C artifact was found (Fig. 3B). Even when the correct product was amplified, the non-template cDNA concentration significantly affected the quantification of the template. The observed starting concentrations showed the expected step-wise decrease per dilution of the template only when 0.4 ng non-template cDNA or more was present in the reaction (Fig. 3C). With less non-template DNA in the reaction, the N_0 values were lower than expected. In a similar experiment, with a 10-fold lower primer concentration the occurrence of amplification artifacts showed similar effects of template and non-template concentrations (Supplemental Figs. 3B-E). Because the observed PCR efficiency was lower more reactions did not show any amplification. However, the C_q values changed proportionally which resulted in correctly estimated target quantities in the reactions with high non-template cDNA input.

3.4. Time-on-bench experiment

Experiments performed to reproduce the effects described above with other templates showed that the occurrence of artifacts is very time-dependent. It takes an experienced technician approximately 2 h to complete the manual pipetting of an entire 384-well qPCR plate leading unavoidably to a variable time-on-bench. To explore this effect a 'time-on-bench' experiment was carried out, in which sets of reactions were left on the bench for 3, 2 and 1 h at room temperature after pipetting of all components in the wells. This experiment showed that after 3 h on the bench all reactions resulted in artifacts whereas after shorter bench times, reactions with enough template input amplified the correct product (Fig. 4A): artifacts started to occur at template concentrations below 15 copies. The fluorescence values observed in the first 3 cycles, when no amplification dependent fluorescence can be detected, were increased in reactions that were left on the bench for 3 h; the highest baseline values were observed in reactions that were leading to the amplification of artifacts (Fig. 4B). Even higher baseline values were observed in the reactions in which the primer and mastermix were left on the bench for 2.5 h before the other reaction components were added, although most of these reactions did not result in artifacts (Fig. 4B). Plateau fluorescence levels were highest in reactions that amplified both products, slightly lower in those that resulted in the correct product and lowest in the reactions that resulted in only artifacts (Fig. 4C); when no amplification occurred the baseline and plateau fluorescence were similar, resulting in a plateau/baseline ratio of close to 1 (Fig. 4D; Supplemental Fig. 4A). For reactions that resulted in a correct product the plateau/baseline ratio ranged between 1.5 and 2 (Fig. 4D). Although the exponential phase, between ground phase noise and the plateau, is determined after baseline subtraction [21] such low plateau/baseline ratios markedly hamper the estimation of the PCR efficiency from the data points in the exponential phase [20]. Indeed, the observed PCR efficiency values per template input and time-on-bench vary considerably between reactions (Fig. 4E). However, on average these PCR efficiency values were independent of the template input and did not differ between the reactions that resulted in correct product, artifacts or both products. Despite these effects of the time-on-bench, the quantification results of the reactions with the correct amplicon showed more or less the expected 10-fold decrease per pDNA dilution step (Supplemental Figs. 4B and C).

3.5. A second fluorescence measurement

Melting peak analysis showed a 7 °C difference in Tm of the correct product (85.5 °C) and the artifact (78.5 °C) in the Cre assay (Supplemental Fig. 4). The profile of the melting peaks showed that the artifact is completely denatured at 82 °C whereas the correct product is still fully double stranded. This property of the assay enabled us to add a short stop to measure fluorescence at 82 °C during the transition of elongation (at 72 °C) to denaturation (at 95 °C), which allowed the measurement of the fluorescence of all products (at 72 °C) and of only the correct product (at 82 °C) in every cycle. This 4-segment cycling protocol was applied in an experiment with a complete Cre-template pDNA − non-template cDNA concentration design with time-on-bench under 2 h. Melting curve analysis showed that amplification of artifacts occurred as observed in earlier experiments (Supplemental Fig. 5A). Artifacts, and reactions without amplification, occurred mainly at low template pDNA concentrations. Fluorescence in the first 3 cycles was 4-fold higher when measured at 72 °C than at 82 °C (Fig. 5A). This result indicates that the baseline fluorescence in qPCR is caused by short, low Tm, double stranded sequences, probably resulting from off-target primer annealing and extension of the Cre primers. The lower baseline fluorescence in the highest template concentration when measured at 82 °C seems to indicate that this a-specific primer annealing and extension is reduced when more template sequences are present (Fig. 5A2). At both measuring temperatures the plateau fluorescence decreased with template input and with the amplification of off-target product (Fig. 5B). Noteworthy, the plateau fluorescence measured at 82 °C is lower than at 72 °C confirming that nonspecific double stranded sequences have been denaturated and do not fluoresce anymore. Indeed, reactions that resulted in amplification of both the correct product and the artifact showed substantially lower plateau fluorescence than reactions that resulted in only correct product (Fig. 5B, cross hatched and orange bars). Reactions that resulted only in artifacts showed plateau levels similar to baseline levels when measured at 82 °C (Fig. 5A2 and B2). The plateau/baseline ratio in the 82 °C measurements was higher than at 72 °C (Fig. 5C) and therefore allowed more precise estimation of PCR efficiency values from the amplification curves (Fig. 5D). The absence of contributions of off-target products, and the more precise PCR efficiency values, made that the variation in the observed starting concentrations (N_0) was significantly less after measurements at 82 °C (Fig. 5E). These quantification results, which are calculated with the mean PCR efficiency of the reactions with the correct product per non-template cDNA concentration at 82 °C, reflected the dilution series better, and for a larger range of template concentrations than those at 72 °C. Strikingly, reactions that resulted in both products (Fig. 5E2, orange/blue dots) and even those that showed predominantly a melting peak for artifacts (Fig. 5E2, orange dots) resulted in expected N_0 values when measured at 82 °C, although those reactions had to be excluded when measured at 72 °C (Fig. 5E1). When the observed C_q values were used to construct standard curves, the

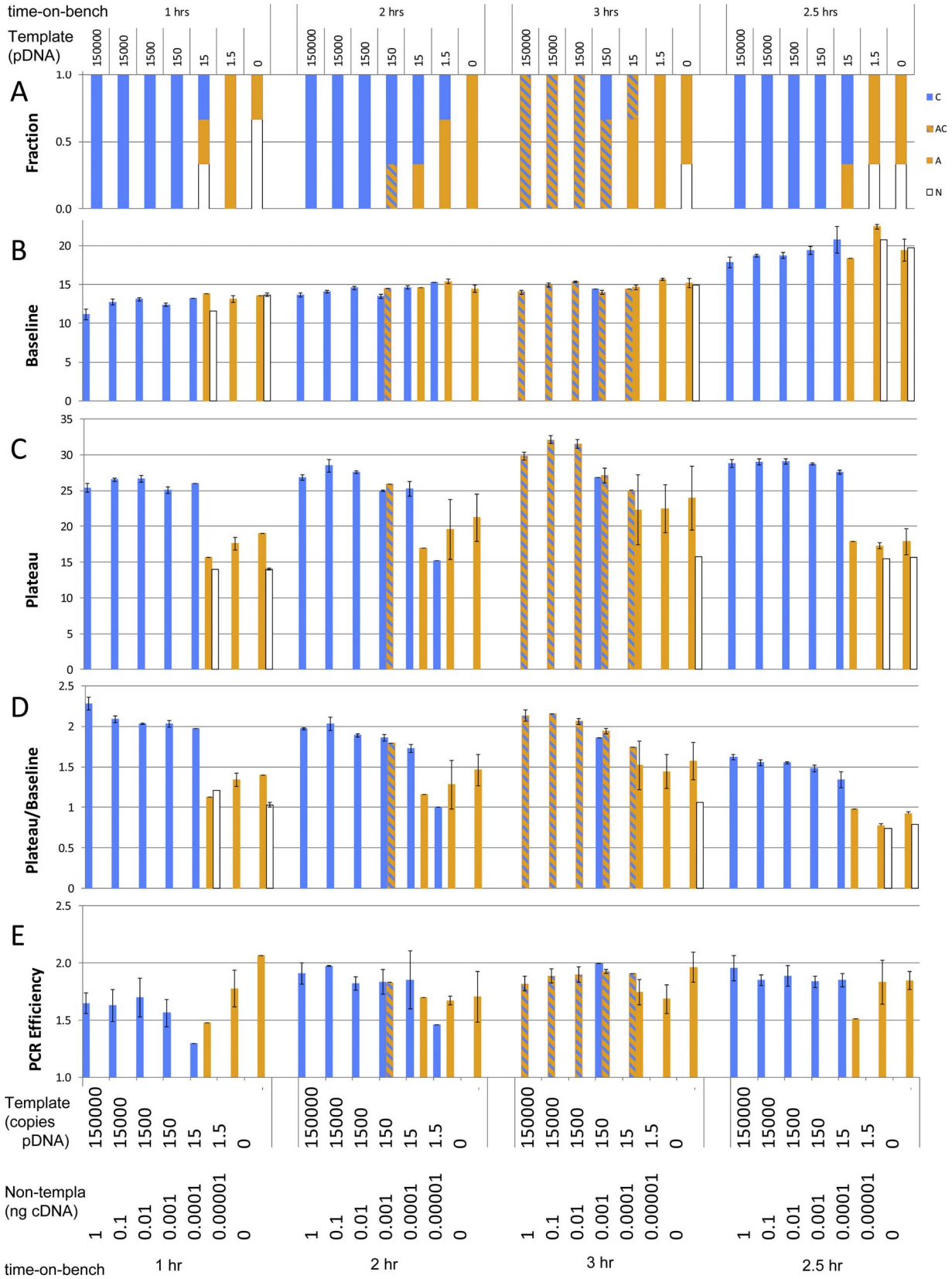

Fig. 4. Characteristics of the amplification curves in a time-on-bench experiment. The PCR plate was left standing on the bench for 1, 2 or 3 h after completion of the pipetting of a set of reactions; the 2.5 h section of the graphs refers to a set of reactions in which only the primers and the master mix were combined. Based on melting peak analysis the reactions were grouped into those resulting in correct product (C), artifact (A), both products (AC), and no amplification (N). **A**: Fraction of PCR reactions per amplification product per template input and time-on-bench. **B**: Baseline fluorescence values calculated as the mean raw fluorescence value in the first 3 cycles. **C**: Plateau fluorescence values calculated as the mean raw fluorescence value in the last 3 cycles. **D**: Plateau/baseline ratio. **E**: PCR efficiency derived from the individual amplification curves. Bars show mean ± SD per amplification product per template input and time-on-bench.

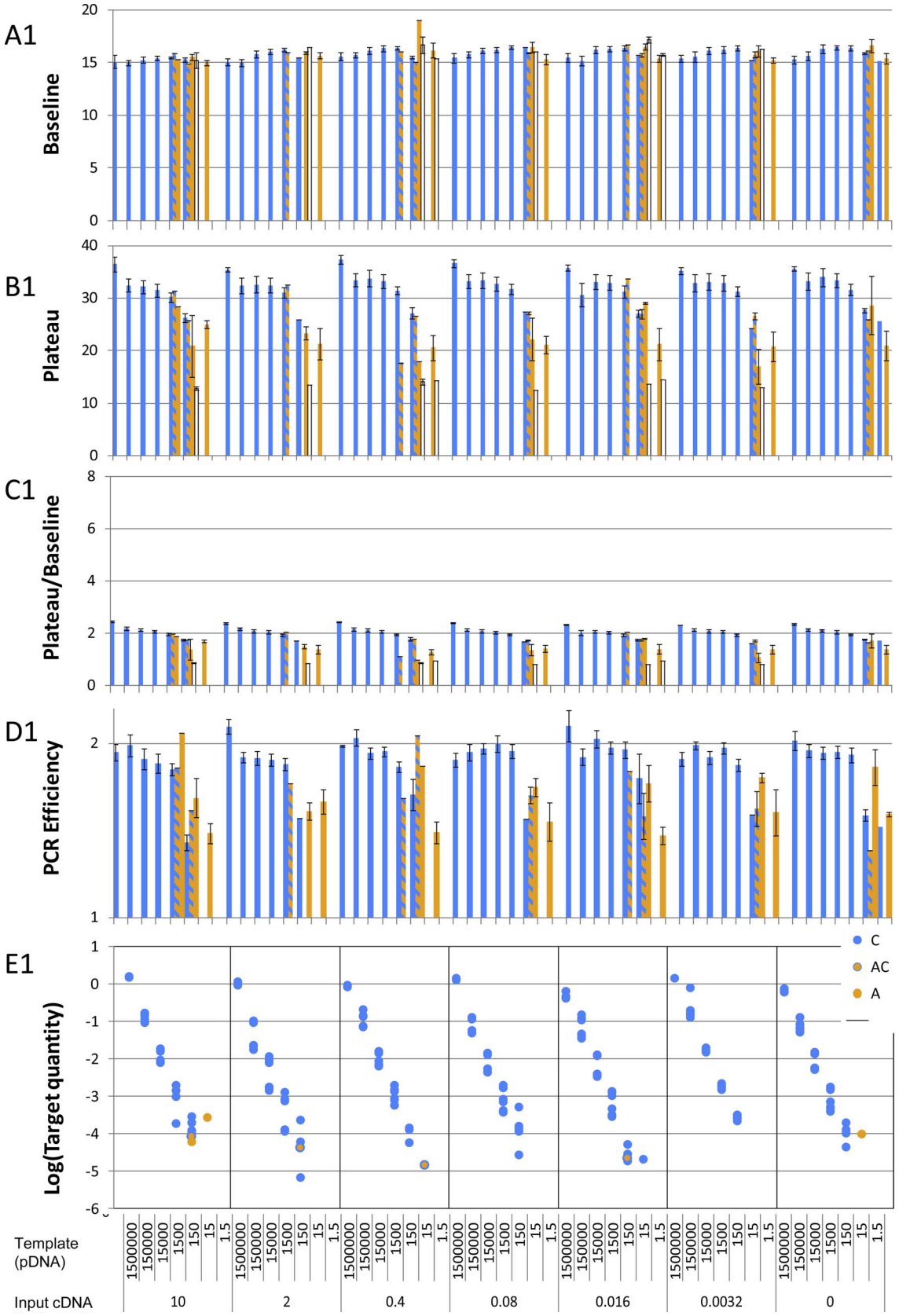

Fig. 5. Effect of measurement temperature an amplification curve characteristics and qPCR results. To avoid the fluorescence contribution of amplification artifacts in an experiment with combinations of template (pDNA) and non-template (cDNA) concentrations monitored with SYBRgreen, fluorescence was measured at the normal 72 °C (panels **1**) and additionally at 82 °C (panels **2**). Based on melting peak analysis the reactions were grouped into those resulting in correct product (C), artifact (A), both products (AC), and no amplification (N: Supplemental Fig. 5A). **A**: Baseline fluorescence level calculated as the mean raw fluorescence value in the first 3 cycles. **B**: plateau fluorescence level calculated as the mean raw fluorescence value in the last 3 cycles. **C**: plateau/baseline ratio. **D**: PCR efficiency determined from individual amplification curves. **E**: Observed target quantity. For each parameter the bars show mean ± SD determined from amplification curves per group of amplification products per template and non-template input. (For interpretation of the references to colour in this figure legend, the reader is referred to the web version of this article.)

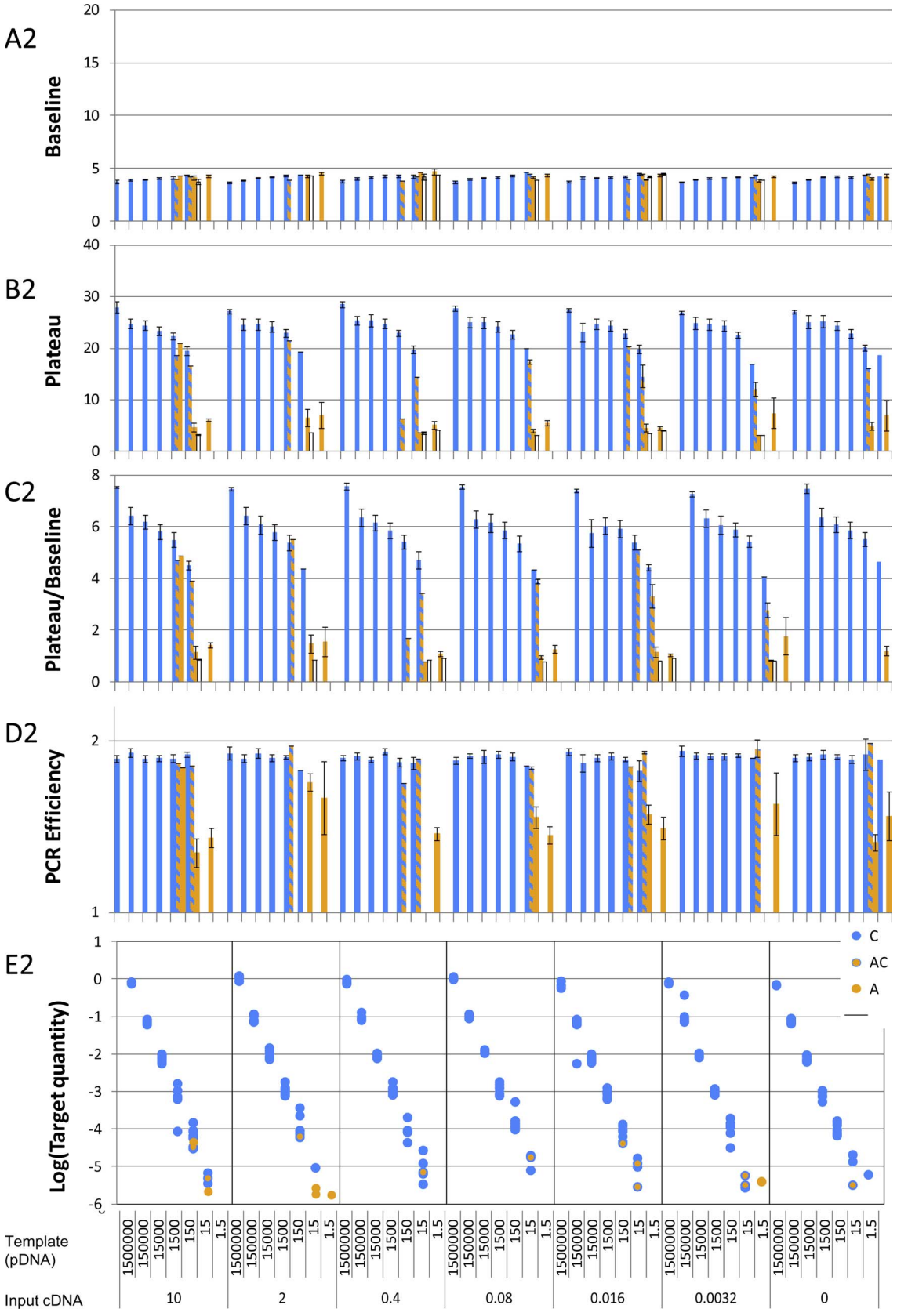

Fig. 5. (*continued*)

measurements at 82 °C resulted in less variable PCR efficiencies [27] (Supplemental Figs. 5B and C).

4. Discussion

The amplification of artifacts is a recurring theme in qPCR literature but the conditions that lead to amplification of such off-target products remains rather elusive. In three different model systems, monitored with intercalating dyes with different PCR systems and master mixes, we encountered artifacts that had either a higher or a lower melting temperature than the targeted product. The analysis of amplification curves, plotted on a logarithmic fluorescence axis can be used to determine the PCR efficiencies of individual reactions [20]. This analysis showed that the observed amplification efficiencies of specific or non-specific products completely overlap. Because both products depend on the annealing of the same pair of primers this is not an unexpected result. Therefore, the shape of the amplification curve cannot be used to assess the specificity of the PCR reaction. The position of the amplification curve, reflected in its C_q value, is thought to give an indication of specificity because high C_q values are more often associated with off-target products. However, a strict cut-off C_q value cannot be defined, but as a rule of thumb and to stay on the safe side, one should use a C_q above 27 as indicative for potential artifact generation. The occurrence of artifacts is dependent on the properties of the master mixes, primer sequences and cycling conditions. Full evaluation of each of these factors is beyond the scope of this paper.

The primer pairs that were used in the evaluation of 93 genes of the Wnt-pathway in chicken embryonic tissues all resulted in the correct product in the positive control tissue (complete chicken embryo) using routine PCR conditions. These individual tissues were processed similarly, resulting in the same type of cDNA. However, when the assays were applied these tissues, which express these genes at different levels, PCR artifacts occurred frequently and mainly independently of the C_q value. These results support the recommendation that users should always check the identity of the amplified product with melting curve analysis, gel electrophoresis and/or sequence analysis [2,3]. When the melting curve analysis shows the amplification of undesired products, the contribution of these products to the observed C_q value is unknown which hampers reliable quantification.

In several cases the melting peak analysis shows that the correct product is found in reactions with a C_q value outside the linear range of a dilution series. This means that the fact that the C_q value is in the range of the negative control cannot, in itself, be used to discard the reaction as nonspecific or negative. The presence of the target and thus correct amplification in low input reactions is determined by Poison probability and the C_q values of such reactions can indeed not be interpreted quantitatively. However, the amplification of the specific product cannot be ignored and the reaction has to be reported as 'target present'.

Nonspecific amplification was shown to be dependent on the concentrations of the primer, template and non-template DNA. The formation of hybrid DNA molecules through jumping between homologous sequences has been extensively discussed in the early days of PCR [12] and is still a concern when pre-amplification of the sample is required, e.g. in massive sequencing [24] and single cell analyses [25]. In this respect, it should also be noted that long PCR products, originating from specific annealing of primers to full length cDNA, make up more than 15% of the amplification products until cycle 6 [26]. Recombination between such extended forward and reverse strands during the first cycles of PCR can be the origin of high melting temperature PCR artifacts. The observation of such artifacts in the MS2 experiments fits with this hypothesis. Moreover, the relatively high baseline values in reactions that were going to result in off-target products indicates that these artifacts may already be present prior to the first PCR cycles and are not only generated later.

The time-on-bench experiment clearly shows that the mixture of primers, template and polymerase present after completion of the pipetting allows interactions that lead to increasing occurrence of artifacts with increasing bench time before the first PCR cycle even with hot-start technology. Although room temperature should keep the polymerase inactive, its residual activity and the extended period at low temperature probably allows for the extension of a-specifically annealed primers and thus the generation of artifacts. The pipetting session and waiting times in the work flow should, therefore, be kept as short as possible and should never be longer than 2 h. To avoid the formation of amplifiable primer-dimers, master mixes containing primers and polymerase should not be prepared too long before the template containing cDNA is added. Especially, in high-throughput experiments using pipetting robots the master mixes are prepared well in advance and plates are pipetted at room temperature. The current findings show that long storage of plates between pipetting and measurement should be avoided.

The absence of template in the no-tissue control reactions, or low template concentrations in highly diluted samples, leads to low melting temperature artifacts, probably primer-dimers. However, the MS2 experiments show that the same annealing temperature and primer concentration can also lead to high melting temperature artifacts when the template DNA is present in relative high concentrations. The abundance of both types of artifacts increased with increasing primer concentration. The recommended primer concentrations are often in the range that resulted in artifacts. When the PCR is monitored with DNA-binding dyes the amplification of a nonspecific product can readily be confused with a positive reaction. With probe-based monitoring of the PCR such artifacts are not observed but can be present and affect the PCR dynamics. Because nonspecific products are easily detected by melting peak analysis, it is recommended that the initial steps of qPCR assay development are performed with DNA-binding dyes and that the probe-based monitoring is implemented when the specificity of the amplification product is validated for the whole range of applications of the assay.

The template/non-template ratio experiments that were performed to further dissect the effect of input on the occurrence of artifacts showed that nonspecific products were formed at low template as well as at low non-template input. Nonspecific amplification thus depends on a 3-way interaction between primer, template and non-template concentrations in the reaction. These experiments showed that the C_q values, and thus observed starting concentrations, of the reactions that resulted in specific products were affected by the concentration of non-template cDNA. The reactions performed correctly and reproducibly when non-template input was between 10 and 0.4 RNA equivalents, commonly used in RT-qPCR experiments. However, at lower non-template input the amplification of the targeted product showed a shift to higher C_q values than expected based on the dilution of the template. This indicates that a minimal amount of carrier DNA is required for valid quantification. An explanation for this observation might be that the total cDNA concentration affects the PCR through its effect on the free water volume as a result of water-caging by DNA; the relative large reaction volume with low carrier concentrations might then negatively affect the PCR conditions. The correct results observed for low template input combined with high non-template input shows that these effects can be avoided by dilution of samples in a fixed amount of non-template carrier DNA.

The Cre-target used in the template − non-template two-way experiment allowed the specific measurement of the amplified target at an increased measurement temperature, in this case at 82 °C instead of 72 °C. The results show that this approach greatly improves the results of the qPCR analysis. The absence of the contribution of off-target products to the observed fluorescence leads to strongly improved plateau/baseline ratios, more precise PCR efficiency estimation and thus to less variable starting concentrations. Even reactions that showed mainly off-target product in the melting curve analysis resulted in a correct starting concentration and could thus be included in further

analysis. Measurement at a high temperature thus improved the sensitivity of the qPCR analysis. To make use of this approach, assays should be designed in such a way that melting temperatures of the desired amplicon and the primer-dimer products differ sufficiently to allow measurement of the targeted amplicon at a temperature at which the artifact is fully denaturated.

Taken together, the current results show that the interpretation of a conventional dilution series experiment should take into account that low template as well as low non-template concentrations may lead to more frequent amplification of nonspecific products. In diluted samples the observation of the signal associated with an amplification product can therefore not be equated to the presence of the specific target in the sample without the positive identification of the product. Not only the random presence of the target in the diluted sample but also off-target amplification has to be taken into account in the interpretation of such diluted reactions and their inclusion in standard curves. This is especially relevant when 'not expressed' or 'not present' are among the possible outcomes of the test as is the case in digital PCR and diagnostic assays. Although primer-dimer artifacts should already be avoided in the design phase of the experiment, avoidance of long bench times and measurement of fluorescence at higher temperature can further help to increase the specificity and sensitivity of a qPCR experiment. However, for assays based on fluorescence monitoring with DNA binding dyes verification of the amplification product with melting curve analysis remains the minimal requirement. This study included a limited number of assays and our results cannot be extrapolated directly to other assays. However, the results should serve as a guide for the variables that have to be considered by developers of in-house qPCR assays. The experiments that we described can serve as examples for the trouble-shooting journey that leads to a validated and robust assay.

Acknowledgements

ARV was supported by CardioNeT, the EU FP7-Marie Curie-ITN actions ITN-GA-2011-289600grant.

Appendix A. Supplementary data

Supplementary data associated with this article can be found, in the online version, at http://dx.doi.org/10.1016/j.bdq.2017.10.001.

References

[1] S.A. Bustin, V. Benes, J. Garson, J. Hellemans, J. Huggett, M. Kubista, et al., The need for transparency and good practices in the qPCR literature, Nat. Methods 10 (11) (2013) 1063–1067, http://dx.doi.org/10.1038/nmeth.2697 (PubMed PMID: 24173381).

[2] S.A. Bustin, V. Benes, J.A. Garson, J. Hellemans, J. Huggett, M. Kubista, et al., The MIQE guidelines: minimum information for publication of quantitative real-time PCR experiments, ClinChem 55 (4) (2009) 611–622.

[3] T. Nolan, R.E. Hands, S.A. Bustin, Quantification of mRNA using real-time RT-PCR, NatProtoc 1 (3) (2006) 1559–1582.

[4] M.A. Poritz, K.M. Ririe, Getting things backwards to prevent primer dimers, The Journal of molecular diagnostics: JMD 16 (2) (2014) 159–162, http://dx.doi.org/10.1016/j.jmoldx.2014.01.001 (PubMed PMID: 24457120).

[5] T. Kanagawa, Bias and artifacts in multitemplate polymerase chain reactions (PCR), J. Biosci. Bioeng. 96 (4) (2003) 317–323, http://dx.doi.org/10.1016/S1389-1723(03)90130-7 (PubMed PMID: 16233530).

[6] Q. Chou, M. Russell, D.E. Birch, J. Raymond, W. Bloch, Prevention of pre-PCR mis-priming and primer dimerization improves low-copy-number amplifications, Nucleic Acids Res. 20 (7) (1992) 1717–1723 (PubMed PMID: 1579465 PubMed Central PMCID: PMC312262).

[7] K. Sachse, Specificity and performance of PCR detection assays for microbial pathogens, Mol. Biotechnol. 26 (1) (2004) 61–80, http://dx.doi.org/10.1385/MB:26:1:61 (PubMed PMID: 14734824).

[8] E.H. Ashrafi, N. Paul, Improved PCR specificity with hot start PCR primers, Biotechniques 47 (3) (2009) 789–790 (PubMed PMID: 19862849).

[9] J. Vandesompele, A. De Paepe, F. Speleman, Elimination of primer-dimer artifacts and genomic coamplification using a two-step SYBR green I real-time RT-PCR, Anal. Biochem. 303 (1) (2002) 95–98, http://dx.doi.org/10.1006/abio.2001.5564 (PubMed PMID: 11906156).

[10] M.L. Wong, J.F. Medrano, Real-time PCR for mRNA quantitation, Biotechniques 39 (1) (2005) 75–85.

[11] G. Ruano, D.E. Brash, K.K. Kidd, The first few cycles, Amplifiations: a Forum for PCR users 7 (1991) 4.

[12] S.J. Odelberg, R.B. Weiss, A. Hata, R. White, Template-switching during DNA synthesis by thermus aquaticus DNA polymerase I, Nucleic Acids Res. 23 (11) (1995) 2049–2057 (PubMed PMID: 7596836 PubMed Central PMCID: PMC306983).

[13] F. Trautinger, C. Jantschitsch, R. Strohal, M. Pourmojib, I. Kindas-Mugge, Mispriming and PCR amplification of hsp27, Cell Stress Chaperones 2 (4) (1997) 276–277 (PubMed PMID: 9495284 PubMed Central PMCID: PMC313006).

[14] A. Malgoyre, S. Banzet, C. Mouret, A.X. Bigard, A. Peinnequin, Quantification of low-expressed mRNA using 5' LNA-containing real-time PCR primers, Biochem. Biophys. Res. Commun. 354 (1) (2007) 246–252, http://dx.doi.org/10.1016/j.bbrc.2006.12.194 (PubMed PMID: 17217915).

[15] S. Lefever, F. Pattyn, J. Hellemans, J. Vandesompele, Single-nucleotide polymorphisms and other mismatches reduce performance of quantitative PCR assays, Clin. Chem. 59 (10) (2013) 1470–1480, http://dx.doi.org/10.1373/clinchem.2013.203653 (PubMed PMID: 24014836).

[16] J. Dreier, M. Stormer, K. Kleesiek, Use of bacteriophage MS2 as an internal control in viral reverse transcription-PCR assays, ournal of clinical microbiology 43 (9) (2005) 4551–4557, http://dx.doi.org/10.1128/JCM.43.9 (PubMed PMID: 16145106; PubMed Central PMCID: PMC1234060).

[17] F.J. de Lange, A.F.M. Moorman, V.M. Christoffels, Atrial cardiomyocyte-specific expression of Cre recombinase driven by an Nppa gene fragment, Genesis 37 (2003) 1–4.

[18] M.W. Pfaffl, T.M. Georgieva, I.P. Georgiev, E. Ontsouka, M. Hageleit, J.W. Blum, Real-time RT-PCR quantification of insulin-like growth factor (IGF)-1, IGF-1 receptor, IGF-2, IGF-2 receptor, insulin receptor, growth hormone receptor, IGF-binding proteins 1, 2 and 3 in the bovine species, Domest. Anim. Endocrinol. 22 (2) (2002) 91–102 (PubMed PMID: 11900967).

[19] C. Zhang, G. Zhang, M. Yang, K. Ben, Elimination of primer-dimer effect in SYBR green I real-time RT-PCR using 4-step program. China, J. Biochem. Mol. Biol. (2004) 387–392.

[20] J.M. Ruijter, C. Ramakers, W.M. Hoogaars, Y. Karlen, O. Bakker, M.J. van den Hoff, et al., Amplification efficiency: linking baseline and bias in the analysis of quantitative PCR data, Nucleic Acids Res. 37 (2009) e45.

[21] J.M. Ruijter, M.W. Pfaffl, S. Zhao, A.N. Spiess, G. Boggy, J. Blom, et al., Evaluation of qPCR curve analysis methods for reliable biomarker discovery: bias, resolution, precision, and implications, Methods 59 (2013) 32–46, http://dx.doi.org/10.1016/j.ymeth.2012.08.011 S1046-2023(12)00229-0 [pii];.

[22] J.M. Ruijter, A. Ruiz-Villalba, J. Hellemans, A. Untergasser, Removal of between-run variation in a multi-plate qPCR experiment, Biomol. Detect. Quantif. 19 (2015) 5 (Epub 04/27/2015).

[23] M.W. de Ronde, J.M. Ruijter, D. Lanfear, A. Bayes-Genis, M. Kok, E. Creemers, et al., Practical data handling pipeline improves performance of qPCR-based circulating miRNA measurements, RNA (2017), http://dx.doi.org/10.1261/rna.059063.116 (PubMed PMID: 28202710).

[24] J.M. Kebschull, A.M. Zador, Sources of PCR-induced distortions in high-throughput sequencing data sets, Nucleic Acids Res. (2015), http://dx.doi.org/10.1093/nar/gkv717 (PubMed PMID 26187991).

[25] S. Islam, A. Zeisel, S. Joost, G. La Manno, P. Zajac, M. Kasper, et al., Quantitative single-cell RNA-seq with unique molecular identifiers, Nat. Methods 11 (2) (2014) 163–166, http://dx.doi.org/10.1038/nmeth.2772 (PubMed PMID: 24363023).

[26] H.K. Nogva, K. Rudi, Potential influence of the first PCR cycles in real-time comparative gene quantifications, Biotechniques 37 (2) (2004) 246–248 (PubMed PMID: 15335216 50-3).

[27] J. Hellemans, G. Mortier, P.A. De, F. Speleman, J. Vandesompele, qBase relative quantification framework and software for management and automated analysis of real-time quantitative PCR data, Genome Biol. 8 (2) (2007) R19, http://dx.doi.org/10.1186/gb-2007-8-2-r19 (gb-2007-8-2-r19 [pii]).